Undergraduate Honors Thesis

A Coupled, Multi-Physics Model of the Automotive Brake System with Focus on Dynamic Torque Prediction

SUBMITTED TO:

The Engineering Honors Committee

As partial requirement for graduation with distinction

in the Department of Mechanical Engineering

119 Hitchcock Hall

College of Engineering

The Ohio State University

Columbus, Ohio 43210

WRITTEN BY:

Jared Liette

1573 Virginia Ave.

Columbus, OH 43212

liette.6@osu.edu

Mechanical Engineering Department

Advisor: R. Singh

November 2009

TABLE OF CONTENTS

ABSTRACT

High speed brake judder is one of the common vibration problems in the automotive industry. Judder has been described as an unacceptable vibration/shake experienced in the vehicle when the brakes are applied. This vibration is generally felt at the steering wheel, seat track, and brake pedal. In severe cases, vibration of the entire chassis has been observed. The phenomenon generally occurs if the vehicle is traveling above a threshold speed (roughly 60 mph); the corresponding maximum vibration level occurs at or around 14 Hz.

The fundamental source of the judder problem is the disc-caliper brake system, specifically the brake torque variations T(t) (BTV) and brake pressure variations P(t) (BPV) occurring within the brake system. Disc thickness variation y(t) (DTV) is attributed as the primary source of T(t) in the mechanical system, but it is possible that the dynamic torque acting structurally on the hydraulic system (or the hydraulic system dynamics in general) introduces an additional contribution or feedback to the T(t) level. The purpose of this research was thus to formulate a coupled mechanical and hydraulic multi-physics disc-caliper brake system model, predict the dynamic torque history T(t), and investigate parameter sensitivity with regards to y(t) and T(t).

A new multi-physics software AMESim Image.Lab (by LMS©) is used to formulate the coupled mechanical and hydraulic system model. Using this dynamic model and a three tier sensitivity analysis of the system parameters, several fundamental questions are posed, investigated, and answered. It is demonstrated that a resonance around 20 Hz exists in the system, that a larger y(t) amplitude induces higher brake torque variations, and that run out creates %60 as much T(t) as y(t) does. Results show that there is a mechanical and hydraulic coupling acting on the 2nd mode (about 20 Hz) of the system, and that the addition of an accumulator into the hydraulic system could possibly reduce the dynamic torque levels.

LIST OF FIGURES

LIST OF TABLES

LIST OF SYMBOLS AND ABBREVIATIONS

A_{pad}	-	Pad/Rotor Contact Area [m^2]
A_{pist}	-	Area of Piston Face [m^2]
A_s	-	State Matrix in State Space
B_s	-	Input Matrix in State Space
BPV	-	Brake Pressure Variations [N/m^2]
BTV	-	Brake Torque Variations [N-m]
CPU	-	Computational
C	-	General Hydraulic Compliance [m^3/Pa]
C_{hyd}	-	Lumped Hydraulic System Compliance [m^3/Pa]
C_s	-	Output Matrix in State Space
c_{gpin}	-	Guide Pin Damping [N-sec/m]
c_{pad}	-	Pad Damping [N-sec/m]
D_s	-	Feedforward Matrix in State Space
DTV	-	Disc Thickness Variations [μm]
DTV_{nom}	-	Nominal Disc Thickness Amplitude [μm]
F_{brake}	-	Brake Force Applied to the Master Cylinder [N]
F_{calp}	-	Caliper Side Pad/Rotor Friction Force [N]
F_{pist}	-	Piston Side Pad/Rotor Friction Force [N]
f.d.f.	-	Frequency Dependent Friction
I	-	General Hydraulic Inertance [Pa-sec^2/m^3]
I_{hyd}	-	Lumped Hydraulic System Inertance [Pa-sec^2/m^3]
I_{eff}	-	Effective Inertia of Rotor Disc [kg-m^2]
k_{calp}	-	Caliper Stiffness [N/m]
k_{fl}	-	Hydraulic Fluid Stiffness [N/m]
k_{hyd}	-	Lumped Hydraulic Stiffness [N/m]
k_{mc}	-	Master Brake Cylinder Stiffness [N/m]
k_{pad}	-	Pad Stiffness [N/m]
k_{pist}	-	Piston Stiffness [N/m]
k_{seal}	-	High Pressure Seal Stiffness [N/m]
M_{Cpad}	-	Caliper Side Brake Pad Mass [kg]
M_{Ppad}	-	Piston Side Brake Pad Mass [kg]
M_{mc}	-	Master Brake Cylinder Mass [kg]

M_{calp}	-	Caliper Mass [kg]
M_{fl}	-	Hydraulic Fluid Mass [kg]
M_{pist}	-	Piston Mass [kg]
M_{rot}	-	Rotor Mass [kg]
N_{calp}	-	Caliper Side Pad/Rotor Normal Force [N]
N_{pist}	-	Piston Side Pad/Rotor Normal Force [N]
P	-	Dynamic Pressure [N/m^2]
P_A	-	Pressure Applied to Hydraulic System [N/m^2]
P_{acc}	-	Accumulator Fluid Pressure [N/m^2]
P_{gas}	-	Accumulator Gas Pre-Charge Pressure [N/m^2]
PP	-	Peak-to-Peak
R	-	General Hydraulic Resistance [Pa-sec/m^3]
R_{eff}	-	Radius from Disc Center to Pad/Rotor Contact [m]
Q	-	Fluid Flow Rate @ Accumulator Orifice [m^3/sec]
R_{hyd}	-	Lumped Hydraulic System Resistance [Pa-sec/m^3]
T	-	Dynamic Torque [N-m]
t	-	Time [sec]
u_s	-	Control Vector in State Space
x_{Cpad}	-	Caliper Side Brake Pad Displacement [m]
x_{Crot}	-	Caliper Side Rotor Displacement [m]
x_{Ppad}	-	Piston Side Brake Pad Displacement [m]
x_{Prot}	-	Piston Side Rotor Displacement [m]
x_{calp}	-	Caliper Displacement [m]
x_{fl}	-	Hydraulic Fluid Displacement [m]
x_{mc}	-	Master Brake Cylinder Displacement [m]
x_{pist}	-	Piston Displacement [m]
x_s	-	State Vector in State Space
y	-	Disc Thickness Variations [m]
y_s	-	Output Vector in State Space
α	-	Disc Rotational Acceleration [rad/sec^2]
μ	-	Pad Coefficient of Friction [null]
Ω	-	Disc Rotational Speed [rad/sec]
τ	-	Dummy Time Variable for Integration [sec]

1. INTRODUCTION

1.1. Motivation and Literature Review

High speed brake judder is one of the common vibration problems in the automotive industry. Judder has been described as an unacceptable vibration/shake experienced in the vehicle when the brakes are applied [1-2]. This vibration is generally felt at the steering wheel, the seat track, and the brake pedal. In severe cases, vibration of the entire chassis has been observed [1]. The phenomenon generally occurs if the vehicle is traveling above a threshold speed (roughly 60 mph); the corresponding maximum vibration level occurs at or around 14 Hz [2].

The fundamental source of the judder problem is the disc-caliper brake system; a typical floating caliper configuration is shown in Figure 1. The brake pads, rotor disc, brake caliper, and pistons represent the mechanical system. The piston chamber and hydraulic lines represent the hydraulic system.

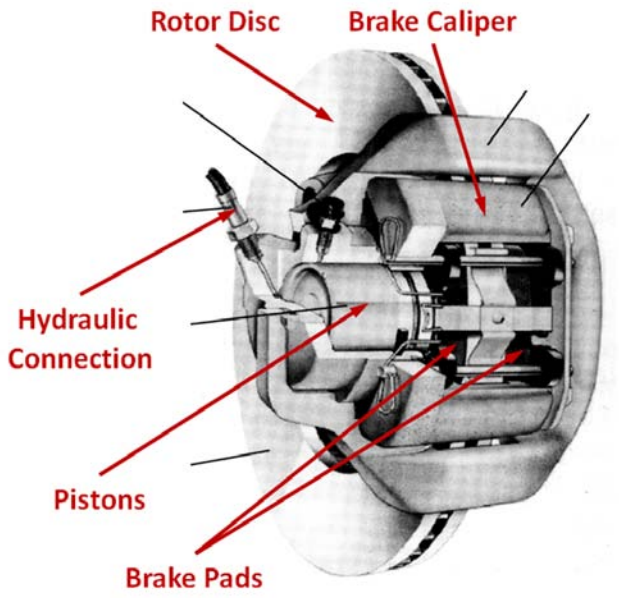

Figure 1: Floating Disc-Caliper Brake Assembly [3]

It is assumed that the sources of the vibration are the brake torque variations T(t) (BTV) and brake pressure variations P(t) (BPV). The main contributors to BTV/BPV seem to be disc thickness variation y(t) (DTV) as well as thermal and wear effects [4]. However, their roles are not well understood; they are also interrelated. Several causes, observed effects, and analysis methods are summarized in reference [5] though this list is not exhaustive. Much of the available literature does not focus on the sources, but rather on "band-aide" modifications to the vehicles that seem to attenuate the observed effects.

The disc thickness variation y(t) is generally on the order of 10 to 20 µm for a given vehicle [5]. It is a result of geometrical irregularities during manufacturing (roughly 5 to 10 µm) as well as uneven rotor wear that can occur during use, e.g. disc runout and uneven corrosion [5]. Thermal effects during the braking event amplify y(t) and T(t), as uneven thermal expansion occurs and hot spots form at peak disc thickness levels. The y(t) can increase by as much as 10 µm at the hot spots [5]. Other effects such as coning and warping of the disc can occur due to the uneven heating, as well as large variations in the pad coefficient of friction during a given braking event [5]. Significant dynamic torques on the order of 100 N-m are then generated [1-2, 4-5]. A schematic of both DTV and runout can be seen in Figure 2, with appropriate labels and descriptions.

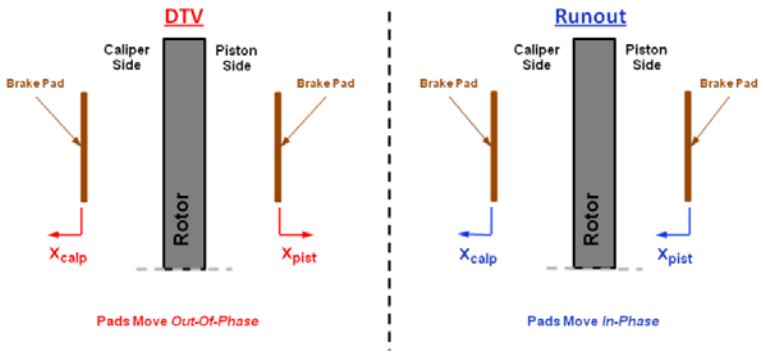

Figure 2: Disc-Caliper Brake Assembly

The complex coupling between disc surface variations (under cold condition) and thermally induced expansions of these variations is yet to be understood. As a result, the cause(s) of T(t) and P(t) and their dependence on y(t) is yet to be properly explained. Without a clear understanding of the sources, brake judder problems have traditionally been solved via empirical methods rather than a clear systematic approach [1-2, 4-5]. Some insight has been provided, but in large part the judder problem remains a mystery.

1.2. Research Goals

It is possible that the dynamic torque acting structurally on the hydraulic system (or the hydraulic system dynamics in general) introduces an additional contribution or feedback to the T(t) level. The purpose of this research has been to formulate a coupled, multi-physics disc-caliper brake system model and predict the dynamic torque history T(t). While the torque history is of interest for a wide variety of situations, the main motivation for this research was high speed brake judder investigation. Both the mechanical and hydraulic components of the brake system are included, with a goal to demonstrate coupling between the two. A simplified schematic of the coupled model is proposed in Figure 2; it is a free caliper, dual piston design.

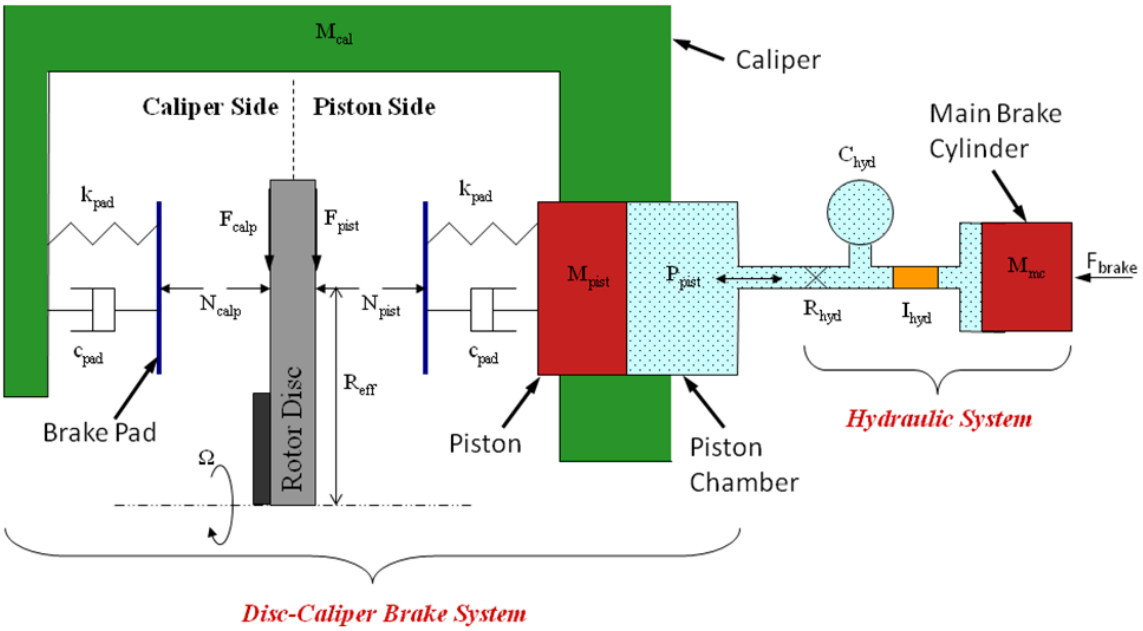

Figure 3: Simplified Disc-Caliper Brake and Coupled Hydraulic Systems

Indeed, a specific aspect that remains unknown in the literature is the correlation between dynamic T(t) and P(t) under judder conditions. It has been suggested by Jacobsson [2, 5] that the two should be proportional as long as the coefficient of friction has very small variations from its mean value [2]. However, experimental data has shown this assumption to be invalid. In fact more T(t) is being generated than expected using prior models [6]. Jacobsson's model [2] consisted of a simple rigid body model of the vehicle as well as a simple mechanical model of the brake system. However, it did not include the hydraulic system. This is indeed the case in the literature reviewed [1-2, 4-5].

The specific goals of this project were as follows:

- Propose an analytical model (such as Figure 2) that can predict dynamic torque T(t) for a given disc thickness y(t) and specified system parameters.

- Examine how T(t) levels change with various hydraulic system parameters (such as fluid compliance) as well as various mechanical parameters (such as caliper stiffness).
- Demonstrate a coupling effect between the mechanical and hydraulic systems.

2. PROBLEM FORMULATION

2.1. Mathematical Formulation

In order to formulate a coupled analytical model of the brake system (Fig. 1), several key system parameters must be identified; these are shown in Figure 2. The caliper mass M_{calp} piston mass M_{pist}, master brake cylinder mass M_{mc}, hydraulic resistance R_{hyd}, hydraulic inertance I_{hyd}, and hydraulic compliance C_{hyd} can be obtained from known material properties and theory. The normal forces applied by the brake pad and the fluid pressure at the piston P_{pist} are calculated iteratively throughout the simulation; the caliper side normal force N_{calp} and piston side normal force N_{pist} both act to slow the rotor. The effective radius R_{eff} from the rotor disc center to the point the normal forces are applied is an estimated constant value.

The coefficient of friction μ for the pad can be determined experimentally as a function of disc speed Ω. For initial modeling purposes, this value was assumed constant. Further, the pad stiffness k_{pad} and damping coefficient c_{pad} must also be determined experimentally; these two values are known to be nonlinear [4]. The stiffness varies with the normal force applied, and the damping coefficient varies with the disc speed. A higher normal force results in a higher stiffness, and a faster speed results in a lower damping coefficient. For initial modeling purposes, these two parameters were assumed constant. Finite element methods and compression tests were utilized to characterize k_{pad} and c_{pad}, as done in literature reviewed [1].

The dynamic brake torque history T(t) is the output of interest from the coupled model. It can be calculated by relating the normal forces on the pad to the frictional forces acting against the rotor movement via the pad coefficient of friction; the caliper side friction force F_{calp} and piston side friction force F_{pist} both act to slow the rotor. The torque can then be found by multiplying the friction forces by the constant radius R_{eff}. The mathematical representation of this can be seen in equation (1).

$$T(t) = R_{eff}\,\mu_{pad}\left\{N_{pist} + N_{calp}\right\} \tag{1}$$

The normal forces are a dependant on many different parameters, from thermal effects to brake pressure variations. Thermal effects are neglected for model simplicity. Other effects such as BPV are calculated iteratively during the simulation and are thus included in the dynamic time history of the normal forces at the brake pad/rotor interface.

2.2. Fundamental Questions

Answers to several fundamental questions were sought as the coupled model evolved. These questions are geared towards achieving the specified goals of the project. They are as follows:

- Does the model show a resonance in the 10 to 20 Hz range that literature associates with brake judder?
- Does the amount of DTV directly relate to the amount of T(t) or BTV?
- Does run out contribute to BTV and to what extent?
- Is there a distinct coupling between the mechanical and hydraulic systems?
- How does adding an accumulator to the hydraulic system affect T(t) or BTV?

2.3. Discretized System Model

A simple linear, lumped parameter model was created for initial system analysis. A schematic of the system can be seen in Figure 4 with components and degrees of freedom labeled. The masses include: The master brake cylinder M_{mc}, the brake fluid M_{fl}, the caliper M_{calp}, the pistons M_{pist}, the caliper side brake pad M_{Cpad}, the piston side brake pad M_{Ppad}, and the rotor M_{rot}. The corresponding degrees of freedom include: The master brake cylinder x_{bc}, the brake fluid x_{fl}, the caliper x_{calp}, the pistons x_{pist}, the caliper side brake pad x_{Cpad}, the piston side brake pad x_{Ppad}, the caliper side rotor surface x_{Crot}, and the piston side rotor surface x_{Prot}. The stiffnesses include: The master brake cylinder k_{bc}, the brake fluid k_{fl}, the high pressure seal k_{seal}, the caliper k_{calp}, the pistons k_{pist}, and the brake pads k_{pad},

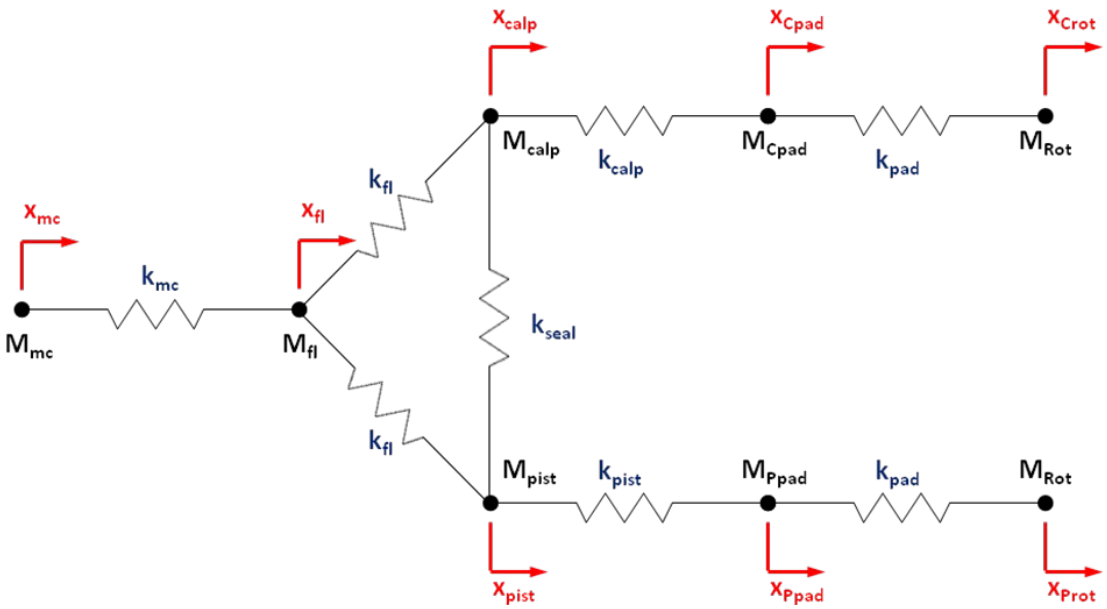

Figure 4: Discrete Linearized Disc-Caliper Brake Model Schematic

The equations of motion for the schematic of Figure 4 can be formulated. There are eight simultaneous ordinary differential equations. For an undamped system, these can be seen in equations (2) through (9).

$$M_{rot}\ddot{x}_{Crot} = -k_{pad}\left(x_{Crot} - x_{Cpad}\right) \tag{2}$$

$$M_{rot}\ddot{x}_{Prot} = -k_{pad}\left(x_{Prot} - x_{Ppad}\right) \tag{3}$$

$$M_{Cpad}\ddot{x}_{Cpad} = k_{pad}\left(x_{Crot} - x_{Crad}\right) - k_{calp}\left(x_{Cpad} - x_{calp}\right) \tag{4}$$

$$M_{Ppad}\ddot{x}_{Ppad} = k_{pad}\left(x_{Prot} - x_{Prad}\right) - k_{pist}\left(x_{Ppad} - x_{pist}\right) \tag{5}$$

$$M_{calp}\ddot{x}_{calp} = k_{calp}\left(x_{Cpad} - x_{calp}\right) - k_{fl}\left(x_{calp} - x_{fl}\right) - k_{seal}\left(x_{calp} - x_{pist}\right) \tag{6}$$

$$M_{pist}\ddot{x}_{pist} = k_{pist}\left(x_{Ppad} - x_{pist}\right) - k_{fl}\left(x_{pist} - x_{fl}\right) - k_{seal}\left(x_{pist} - x_{calp}\right) \tag{7}$$

$$M_{fl}\ddot{x}_{fl} = k_{fl}\left(x_{calp} - x_{fl}\right) - k_{fl}\left(x_{fl} - x_{pist}\right) - k_{mc}\left(x_{fl} - x_{mc}\right) \tag{8}$$

$$M_{mc}\ddot{x}_{mc} = -k_{mc}\left(x_{mc} - x_{fl}\right) \tag{9}$$

For calculations purposes, the equations of motion can be put into matrix form with a corresponding stiffness matrix [K], mass matrix [M], and displacement vector {X}. The internal forces in the system are represented by a force vector {F}. The matrices and vectors can be seen in equations (10) through (13).

$$[\mathrm{K}] = \begin{bmatrix} k_{pad} & 0 & -k_{pad} & 0 & 0 & 0 & 0 & 0 \\ 0 & k_{pad} & 0 & -k_{pad} & 0 & 0 & 0 & 0 \\ -k_{pad} & 0 & k_{pad}+k_{calp} & 0 & -k_{calp} & 0 & 0 & 0 \\ 0 & -k_{pad} & 0 & k_{pad}+k_{pist} & 0 & -k_{pist} & 0 & 0 \\ 0 & 0 & -k_{calp} & 0 & k_{calp}+k_{fl}+k_{seal} & -k_{seal} & -k_{fl} & 0 \\ 0 & 0 & 0 & -k_{pist} & -k_{seal} & k_{pist}+k_{fl}+k_{seal} & -k_{fl} & 0 \\ 0 & 0 & 0 & 0 & -k_{fl} & -k_{fl} & k_{fl}+k_{mc} & -k_{mc} \\ 0 & 0 & 0 & 0 & 0 & 0 & -k_{mc} & k_{mc} \end{bmatrix} \tag{10}$$

$$[\mathrm{M}] = \begin{bmatrix} M_{rot} & 0 & 0 & 0 & 0 & 0 & 0 & 0 \\ 0 & M_{rot} & 0 & 0 & 0 & 0 & 0 & 0 \\ 0 & 0 & M_{Cpad} & 0 & 0 & 0 & 0 & 0 \\ 0 & 0 & 0 & M_{Ppad} & 0 & 0 & 0 & 0 \\ 0 & 0 & 0 & 0 & M_{calp} & 0 & 0 & 0 \\ 0 & 0 & 0 & 0 & 0 & M_{pist} & 0 & 0 \\ 0 & 0 & 0 & 0 & 0 & 0 & M_{fl} & 0 \\ 0 & 0 & 0 & 0 & 0 & 0 & 0 & M_{mc} \end{bmatrix} \tag{11}$$

$$\{X\} = \begin{Bmatrix} x_{Crot} \\ x_{Prot} \\ x_{Cpad} \\ x_{Ppad} \\ x_{calp} \\ x_{pist} \\ x_{fl} \\ x_{mc} \end{Bmatrix} \quad (12) \qquad \{F\} = \begin{Bmatrix} N_{calp} \\ N_{pist} \\ 0 \\ 0 \\ 0 \\ 0 \\ 0 \\ F_{brake} \end{Bmatrix} \quad (13)$$

The rotor displacements x_{Crot} and x_{Prot} are assumed sinusoidal inputs into the system with frequency Ω (the rotor angular velocity). The master brake cylinder displacement x_{bc} is an assumed sinusoidal input with zero magnitude; F_{brake} is thus zero as well. A matrix formulation can thus represent the system in the frequency domain for the undamped system and is seen in equation (14); steady response {X} at any frequency can be solved for via the matrix inversion process, as seen in equation (15). The result is eight equations with eight unknowns. All unknown displacements can first be solved using equation (15), and the internal (constraint) forces can then be solved with equations (14 and 15).

$$\left[-\Omega^2[\mathrm{M}]+[\mathrm{K}]\right]\{\mathrm{X}\} = \{F\} \quad (14)$$

$$\{\mathrm{X}\} = \left[-\Omega^2[\mathrm{M}]+[\mathrm{K}]\right]^{-1}\{F\} \quad (15)$$

While such a formulation can provide reasonable solutions for mechanical systems, there are certain limitations in modeling hydraulic systems. For instance, analogous equations of motion would describe the momentum equations for lumped hydraulic stiffness components but not the continuity equation. In order to better capture the effects of the hydraulic system and identify mechanical and hydraulic coupling, an alternate modeling approach was sought. This is the prime motivation for using the multi-physics AMESim software.

2.4. AMESim Modeling Procedure

In general, the most pragmatic modeling solution was sought for all components involved in the coupled model, balancing a need for computational complexity, solution time (CPU time), and yet realistic component representation.

The initial model created started with as simple a system as could be formulated while still representing the coupled system. Complexities were added as needed to improve the fidelity, with a CPU time check after each modification. In this manner, the current model contains much detail while keeping a CPU time low enough for practical model use and sensitivity analysis.

A discretization method was used to identify key system parameters, such as lumped stiffness, mass, and damping values for the mechanical components (in terms of force and displacements). The hydraulic components were broken up into discretized nodes with pressure and flow rate variables. These nodes are connected by lumped elements with associated fluid compliance, inertance, and resistance values. A lumped parameter method such as this allows for simpler models that can be used to analyze systems with reasonable accuracy.

An additional advantage to a lumped parameter discretization method is easy parameter identification and sensitivity analysis. Experimental methods such as compressibility tests or finite element software packages can be used to obtain lumped mechanical parameters. Basic material properties and component dimensions can also be easily utilized to calculate lumped parameter values using known theory.

3. OVERVIEW OF MULTI-PHYSICS SOFTWARE (AMESim)

3.1. AMESim Capabilities

AMESim is relatively new multi-physics software package created by LMS International© [7]. Models with mechanical, hydraulic, electrical, pneumatic, and thermal elements (and their combinations) can all be combined seamlessly in an easy to use interface. AMESim assumes lumped component, discretized system parameters and is capable of 1D modeling. While this does have some limitations, many practical systems can be formulated in terms of linear and nonlinear components.

Analysis can be done in both the time and frequency domains within AMESim. Time domain analysis is the standard output of numerical integration, and can be done on any variable that varies with time. AMESim stores the time histories for forces, displacements, velocities, pressures, flow rates, etc. Analysis can be done by simply grabbing the desired output from an element and dragging it into the main screen.

Frequency domain analysis is also relatively easy to do in AMESim. The user must specify a time when one expects the system to be at steady state; operating points must then be defined to linearize the system. The user must also define the control variable(s) and state variable(s) to be used in the equations. AMESim then uses a state space formulation to compute the eigenvalues and eigenvectors of the system. Eigenvalues are then computed within AMESim and retrieved via one mouse click. The general state space (first order system) form is shown in equation (16), where $u_s(t)$ contains the control variables, $x_s(t)$ contains the state variables, and $y_s(t)$ contains the output variables. Here A_s represents the state matrix, B_s

represents the input matrix, C_s represents the output matrix, and D_s represents the feedforward matrix.

$$\begin{aligned} \dot{x}_s(t) &= A_s(t)x_s(t) + B_s(t)u_s(t) \\ y_s(t) &= C_s(t)x_s(t) + D_s(t)u_s(t) \end{aligned} \tag{16}$$

The mode shapes at each eigenvalue can also be observed, showing the relative movement of different components to each other. The user can select any of the system's eigenvalues and retrieve a graphical representation of the modal shapes; only the state variables are included in the modal analysis. While this feature of AMESim was not utilized in this study, the numerical eigenvalues and time domain analysis were used extensively.

3.2. AMESim Components

Standard discretized components such as stiffness elements, dampers, masses, pressure sources, hydraulic lines, etc. are the basic components used within AMESim. These components can be connected together in the same manner one would draw a diagram of a system; there is no need to write the equations of motion and create a flow diagram as in Simulink. A sample of these elements can be seen in Figure 5**.**

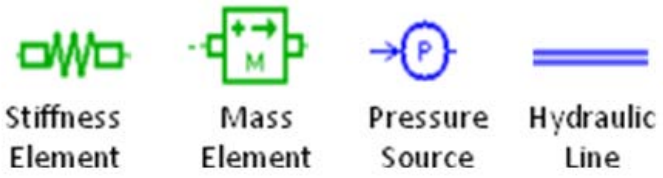

Figure 5: Basic AMESim Components

Most simple models can be created from only these basic components. However, AMESim also has a large collection of super-components available. Throughout the development of AMESim Image.Lab [7], many companies and research organizations Beta tested the software and created complex models using the basic AMESim components. These components were tested and verified experimentally by users and shared with LMS©. As a result, the AMESim component library has slowly grown to include many complicated "super-components" available to all users. These models range from relatively simple things such as piston chambers to complex mechanisms such as kinematic tire analysis models.

It should be noted that this software is only a tool (like other software codes) and it is up to the user to use it intelligently. The easy to use interface and realistic components relieve the burden of writing out the full set of dynamic equations for a given system, but inaccurate results can be obtained if the user does not understand the physics and dynamics behind the components. Extensive help files are available within AMESim, describing the physics and mathematics incorporated in to every element.

4. COUPLED BRAKE SYSTEM MODEL

4.1. Model Assumptions

Several key assumptions were made in the formulation of the coupled hydraulic and mechanical disc-caliper brake system. As mentioned, the model assumes discrete, lumped parameters for all components. Also, the model is limited to 1D analysis based on the AMESim multi-physics software used. It should be noted that the dynamic torque can still be calculated within AMESim without the inclusion of torsional dynamics; the effective inertia of the disc is the only torsional characteristic considered. The inertia is used to calculated the angular

acceleration α(t) of the rotor disc via equation (17), which is turn used to calculate the angular velocity Ω(t) of the rotor disc via equation (18).

$$\alpha(t) = \frac{-T(t)}{I_{eff}} \tag{17}$$

$$\Omega(t) = \int_0^{\Delta t} \alpha(\tau) d\tau \tag{18}$$

It is assumed that both the pad coefficient of friction μ and the effective radius from the disc center to the pad/rotor contact R_{eff} are constant values for model simplicity. It is known from literature that these two values could vary throughout a given braking event [4]; however, determining the manner in which they vary is difficult and will be left to future work. AMESim does allow these two parameters to vary nonlinearly, but it must be supplied by the user.

The disc thickness variation y(t) was assumed to be the input (displacement excitation) into the model. A simple sine wave is used to model the DTV. The wave is 1st order with no contributions from the harmonics; the amplitude is equal to 20μm. Literature suggests that the amplitude of the sine wave (in spatial domain) could vary throughout the braking event as thermal effects take effect, creating hotspots on the rotor [4]. For model simplicity, the thermal effects are neglected. Inclusions of these are left to future work.

4.2. Coupled Model Overview

The full AMESim model created can be seen in Figure 6. It should be noted that the components are color coded: Green being mechanical; blue being fluid; dark red being hydraulic

super-components; and red being signals, controls, and observers. The full model with the brake system main components labeled can be seen in Figure 7.

In general the inputs to the system come from the pressure applied $P_A(t)$ and the pad displacement y(t); the simulation is given a prescribed pressure input, initial DTV level, and initial rotor speed. All other components in the system react to these inputs and iteratively calculate resulting forces, displacements, pressures, etc. The dynamic torque T(t) is also calculated iteratively in the rotor kinematics block and applied to the effective rotor inertia I_{eff}, thus slowing it down and altering the frequency of the DTV sine wave. This cycle repeats iteratively until the simulation time has commenced.

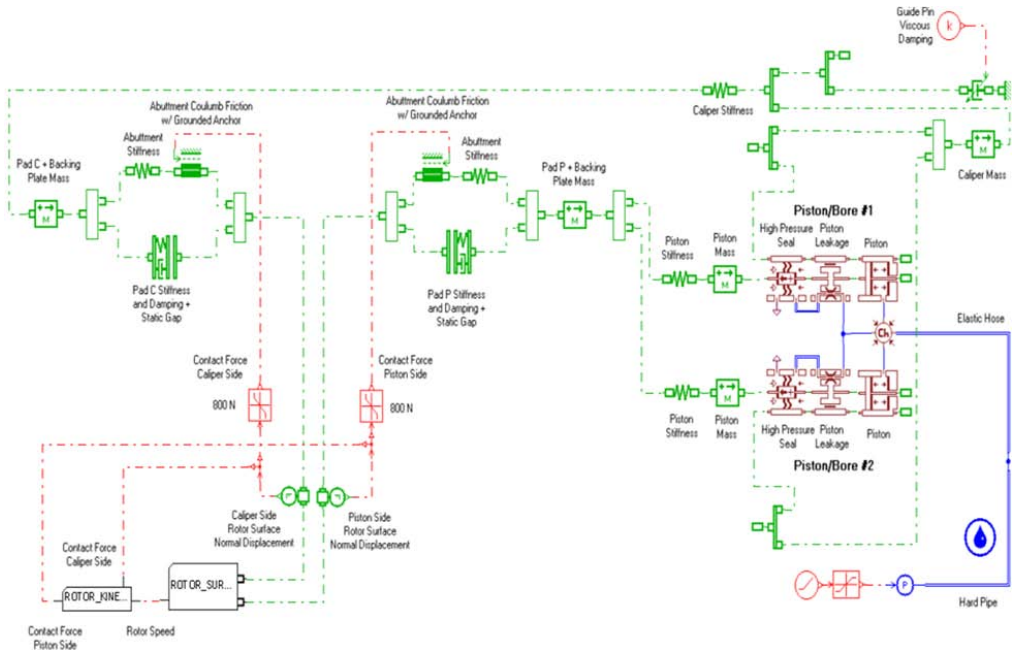

Figure 6: Full AMESim Model

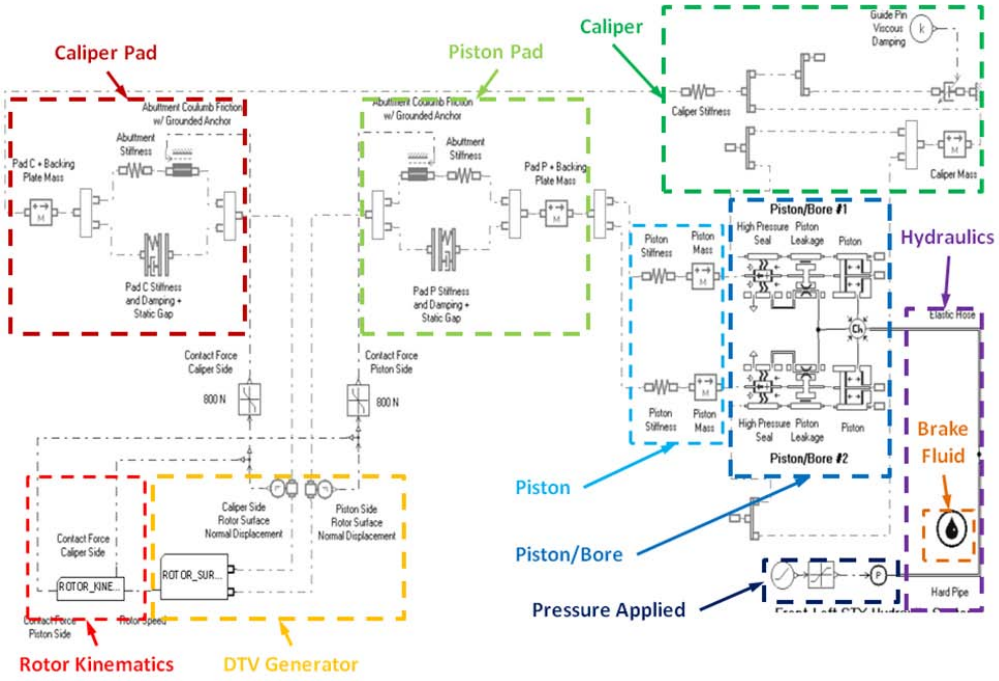

Figure 7: Full AMESim Model with Component Breakdown

4.3. Mechanical Models

A close up of the AMESim model for the rotor kinematics can be seen in Figure 8. Here the iteratively calculated N_{pad} and N_{calp} are used to calculate the dynamic torque T(t) using equation (1). That torque is then applied to the effective inertia of the rotor I_{eff}, which is given an initial velocity. The angular deceleration α(t) is calculated using the simple dynamic equation seen back in equation (17); the angular velocity Ω(t) is found via integration using equation (18). The initial velocity is 25 Hz and decelerates down to 0 Hz.

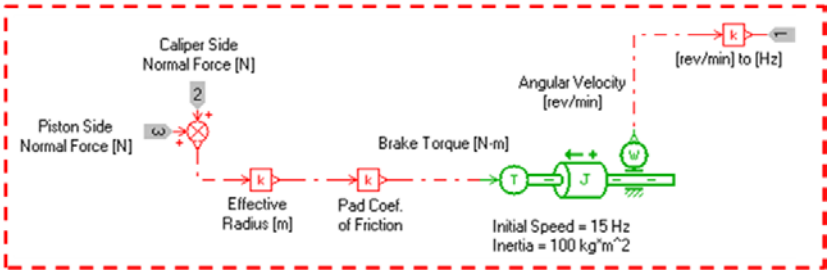

Figure 8: Rotor Kinematics - AMESim Model

A close up of the AMESim model for the rotor surface can be seen in Figure 9. The displacement y(t) is modeled by a 1st order, variable frequency sine wave; the frequency is equal to the angular velocity of the rotor. The amplitude of the sign wave is input as a separate parameter; it is the nominal DTV level DTV_{nom}.

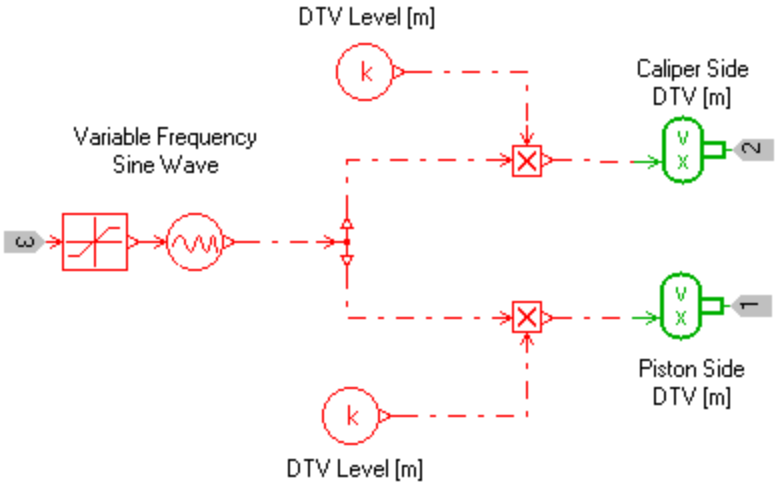

Figure 9: DTV Generator - AMESim Model

The caliper side brake pad and piston side brake pad are fed independent 1st order sign waves. The sine wave describing DTV can be seen in equation (19) with Ω(t) being the disc angular velocity; Ω(t) sweeps from 25 Hz to 0 Hz. A sample value of DTV_{nom} is on the order of 20μm.

$$y(t) = (DTV_{nom}) \sin\{\Omega(t) * t\} \tag{19}$$

A close up of the AMESim model for the caliper side brake pad can be seen in Figure 10; the piston side brake pad is modeled in the exact same manner. The pad is represented by single lumped stiffness, damping, and mass elements.

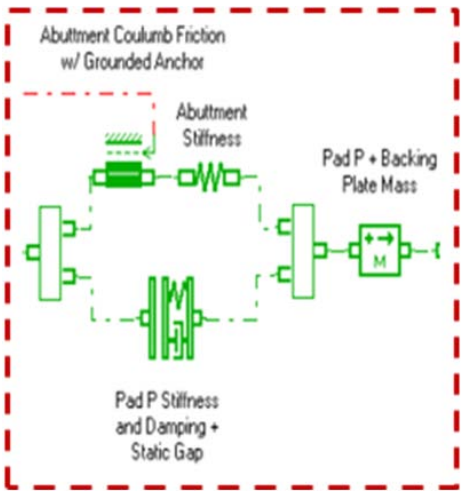

Figure 10: Caliper Side Brake Pad – AMESim Model

Additional parameters included are the static gap between the rotor and pad present initially before the brakes are applied, as well as the abutment stiffness. The abutment stiffness represents the contact between the brake pad and the caliper anchor bracket; it is modeled by a representative stiffness value and Coulomb friction force. A picture of the anchor bracket, brake pad, caliper body, and abutment stiffness can be seen in Figure 11; the components are labeled appropriately.

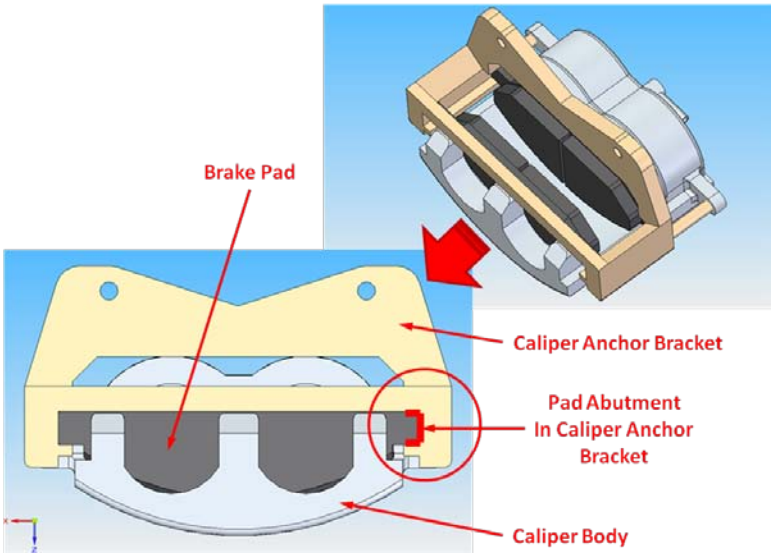

Figure 11: Knuckle, Brake Pad, and Abutment Stiffness w/ Appropriate Labels

A close up of the AMESim model for the caliper body can be seen in Figure 12. It is represented by lumped stiffness and mass elements. Two guide pins attach the caliper body to the anchor bracket. The frictional forces created in these pins are modeled by a simple, constant viscous damping element.

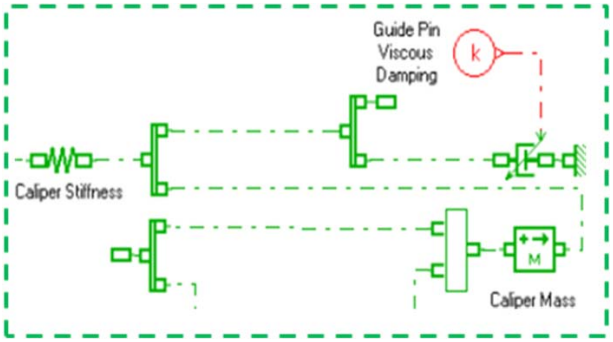

Figure 12: Caliper Body – AMESim Model

A close up of the AMESim model for the pistons can be seen in Figure 13. Each piston is modeled independently with representative lumped stiffness and mass elements. The parameters are the same for both pistons.

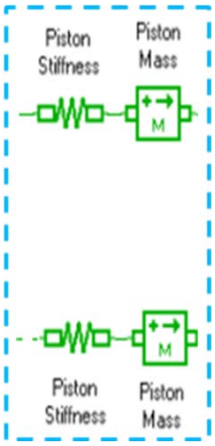

Figure 13: Pistons – AMESim Model

4.4. Hydraulic Models

A close up of the AMESim model for the piston/bore chambers can be seen in Figure 14; a schematic is also shown. The volume of the two chambers is lumped into one element, which includes the expansion of the chamber. Each piston/bore is then modeled in an identical fashion, taking into account the viscous fluid friction, the leakage between the piston/bore interface, and the flexibility of the high pressure seal containing the high pressure brake fluid.

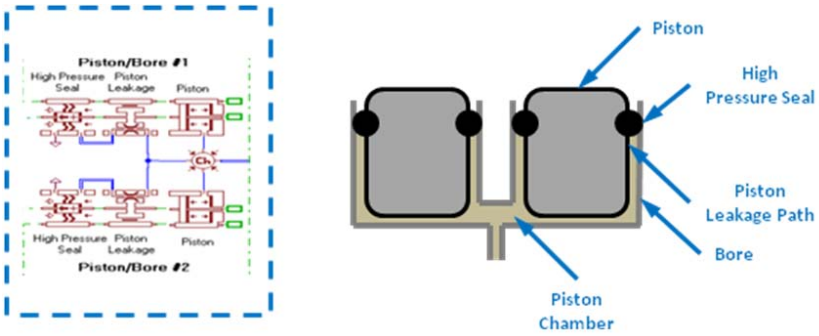

Figure 14: Piston/Bore Chambers – AMESim Model & Schematic

A close up of the AMESim model for the hydraulic lines can be seen in Figure 15. The hard pipe lines and elastic hoses are modeled separately in order to capture the different compliance levels; the elasticity of the material is directly input into the element. The diameter and length of each hydraulic line are also inputs.

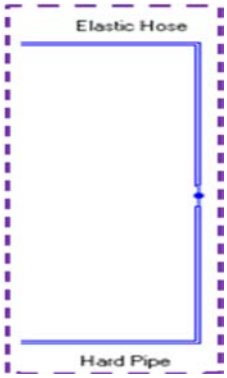

Figure 15: Hydraulic Lines – AMESim Model

A close up of the AMESim model for the hydraulic brake fluid can be seen in Figure 16. Within this element, fluid properties such as density, bulk modulus, absolute viscosity, and air/gas content are prescribed by the user. The user can then select which hydraulic lines to use this fluid in. All lines in the AMESim model use one fluid; it is modeled after an industry standard brake fluid.

Figure 16: Hydraulic Brake Fluid – AMESim Model

A close up of the AMESim model for the pressure applied $P_A(t)$ can be seen in Figure 17. The pressure is modeled as a simple ramp input simulating human application of the brakes, capped by a limit or saturation pressure level. $P_A(t)$ is input directly into the hydraulic lines.

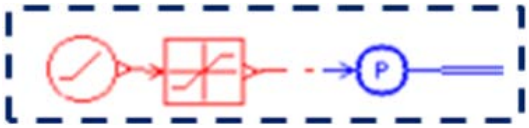

Figure 17: Pressure Applied – AMESim Model

4.5. Simulation Inputs, Outputs, and Initial Conditions

The two inputs into the system are the disc thickness variation y(t) on the rotor surface and the pressure applied to the hydraulic system $P_A(t)$. The y(t) input is a first order sine wave with a variable frequency equal to that of the rotor disc angular speed Ω(t); it is input into the piston and caliper side brake pads independently. The $P_A(t)$ input is a ramp function with a saturation level at a prescribed pressure; the ramp corresponds to suppression of the brake pedal. Both inputs can be seen in graphical form in Figure 18.

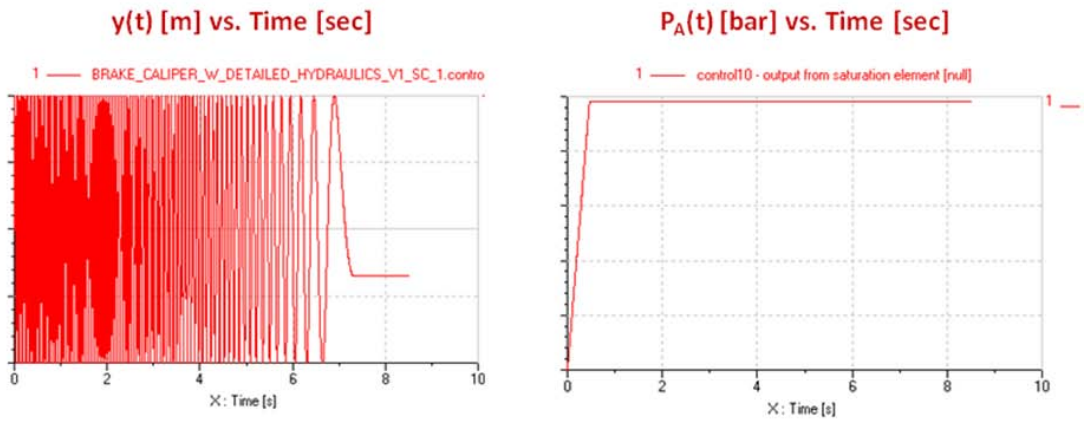

Figure 18: AMESim Model Inputs – y(t) and $P_A(t)$

The only initial condition imposed on the system is the angular velocity of the rotor disc; it corresponds to the initial velocity of the vehicle. The main output of interest is the time history T(t) applied to the rotor disc, as described by equation (1).

4.6. Eigenvalue Model

The AMESim model used for the eigenvalue analysis can be seen in Figure 19. In order to calculate the eigenvalues, the model must be linearized about an operating point at a specific steady state time. Thus, the only input into the system is the pressure applied $P_A(t)$, and the displacement y(t) is disregarded; the system stabilizes quickly. Such an adjustment has no effect on the eigenvalues, as they are a property of the linearized system itself and not the inputs.

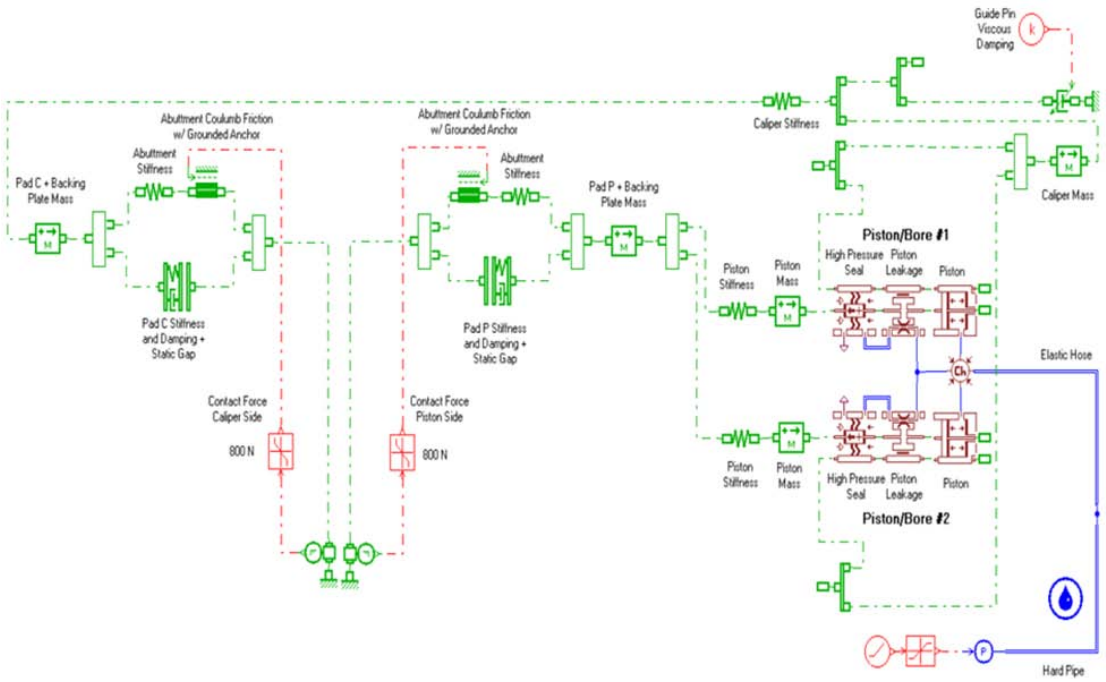

Figure 19: Eigenvalue AMESim Model

5. RESULTS AND DISCUSSION

5.1. Hydraulic Line Model Selection

An important component that needed to be characterized within the coupled model was the hydraulic lines. AMESim has a wide variety of options that take into account different effects including line compressibility, fluid flow friction, line resistance, fluid inertia, and wave equation resonances. As more of these effects are included, the CPU time for the model will start to grow.

Aside from the specific mathematics involved in some of these effects, the various models also consider different fundamental fluid properties such as inertia (I), resistance(R), and compliance (C); the boundary conditions also vary. Table 1 summarized the different models

and the fluid properties included; f.d.f. is defined as frequency dependant friction. The properties are listed as they are considered along the hose, with the left and right most properties being the boundary conditions. The complexity of the model is also noted.

Table 1: Hydraulic Line Model Overview

Submodel	Fluid Properties Considered	Complexity
Compressibility + Friction	R-C-R	Least
Simple Wave Equation	IR-C-IR	↓
Simple *f.d.f. Wave Equation	IR-C-IR	↓
Distributive Wave Equation	IR-C-IR-C-IR-C-IR-C-IR-C-IR-C-IR	↓
Most Complex Wave Equation	IR-C-IR-C-IR-C-……..-C-IR-C-IR-C-IR	Most

For the AMESim hydraulic line, it is assumed that the most complex model is also the most accurate. Thus, the accuracy of the rest will be judged based on how well they coincide with the "Most Complex Wave Equation" output.

5.2. Hydraulic Line Model Options – No Fluid Inertia

The only model considered that does not include fluid inertia is the "Compressibility + Friction" model. As the name suggests, only line compressibility and fluid flow friction are considered. The normalized dynamic torque T(t) output using this model can be seen in Figure 20.

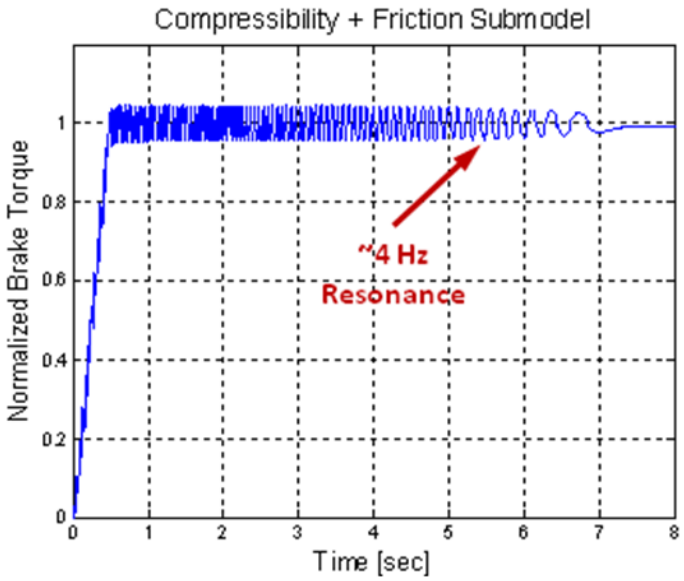

Figure 20: Compressibility + Friction Hydraulic Line Model T(t) Output

An eigenvalue analysis revealed a resonance at roughly 4 Hz within the 25 to 0 Hz sweep that the rotor disc moves through. A resulting peak in the dynamic torque T(t) is evident.

5.3. Hydraulic Line Model Options – With Fluid Inertia

The most basic model considered that takes into account fluid inertia was the "Simple Wave Equation" model. It includes the line compressibility and fluid flow friction as well as fluid inertia. The natural frequency of the fluid mass and column stiffness is considered using the wave equation. The simple wave equation combines the fluid continuity equation with conservation of mass in order to relate fluid flow to pressure. The normalized dynamic torque T(t) output for this model can be seen in Figure 21.

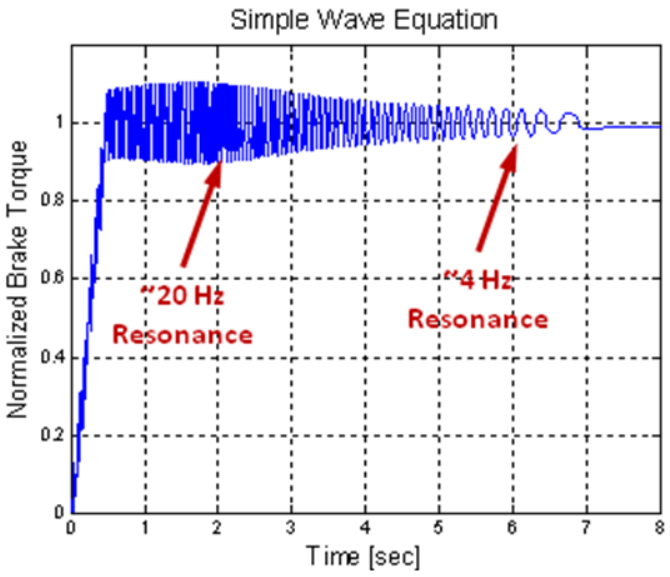

Figure 21: Basic Wave Equation Hydraulic Line Model T(t) Output

An eigenvalue analysis revealed a resonance at roughly 4 Hz as well as 20 Hz within the 25 to 0 Hz sweep that the rotor disc moves through. Two resulting peaks in the dynamic torque T(t) are evident. Based on these results, inertia effects of the fluid need to be considered to fully capture the frequency response of the system.

Three other models considering fluid inertia were analyzed. The "Simple f.d.f Wave Equation" models the fluid inertia in the same manner as the "Simple Wave Equation" model, but considers a frequency dependant fluid friction (f.d.f.) calculation. The "Distributive Wave Equation" model simply adds more nodes in between the boundary conditions, as can be seen from Table 1. The "Complex Wave Equation" also adds more nodes, but uses a much more complicated version of the wave equation than the other models discussed. All three additional inertia models have a similar T(t) output to that of the "Basic Wave Equation" model. An eigenvalue analysis was needed to discern the variation between them.

5.4. Summary of Hydraulic Line Model Selection

The resonance at roughly 4 Hz is the 1st mode of the coupled system; the resonance at roughly 20 Hz is the 2nd mode. The values for these are summarized in Table 2 for each model examined, as well as the corresponding CPU time.

Table 2: Hydraulic Line Model Summary

Submodel	CPU Time [sec]	1st Mode [Hz]	2nd Mode [Hz]
Compressibility + Friction	4.5	3.8	N/A
Simple Wave Equation	9.6	4.0	20.0
Simple f.d.f. Wave Equation	11.6	4.1	19.4
Distributive Wave Equation	718.1	4.0	19.8
Most Complex Wave Equation	1153.9	4.1	19.3

The most pragmatic solution was sought, achieving a low CPU time as well as a similar output to that of the "Most Complex Wave Equation" model. The model best suited is thus the "Simple f.d.f. Wave Equation" model. The first two modes are nearly identical to the most complicated model while maintaining a CPU comparable to the "Simple Wave Equation" model, which is the simplest model considering fluid inertia.

5.5. High Pressure Seal

Two separate AMESim models were considered for the high pressure seal, which is located within the piston/bore chambers. The initial model considered was for a moving hydraulic seal type, i.e. the piston and bore are both allowed to translate along the edge of the seal. There is no fixed connection between the components, only a friction force at the contact areas. The model also assumes pressurized hydraulic fluid on both sides of the seal.

Further investigation into an actual piston/bore chamber component revealed a different scenario than what was being described by the moving seal model. The high pressure seal actually sits within a groove machined into the bore surface, forming a fixed connection between the two. Also, one side of the seal is exposed to pressurized fluid while the other is exposed to atmospheric air.

Thus, a different model within AMESim was pursued to properly model the high pressure seal. A diaphragm type model was selected, as the bore/seal connection is similar to how a diaphragm connects to a surface, forming a pivot point between the diaphragm/seal and connection point. It also assumes pressurized fluid on one side of the seal and atmospheric air on the other.

5.6. High Pressure Seal – Pad/Rotor Normal Forces

Aside from the assumed conditions for the models, N_{pist} and N_{calp} are also drastically different between the two. The moving seal type model computes the mean values to be nearly identical with the vibratory portion of N_{pist} to be larger, while the diaphragm type model computes the mean and vibratory portions of $N_{;ist}$ to be larger than that of N_{calp}. The normalized force time histories can be seen in Figure 22 for both models.

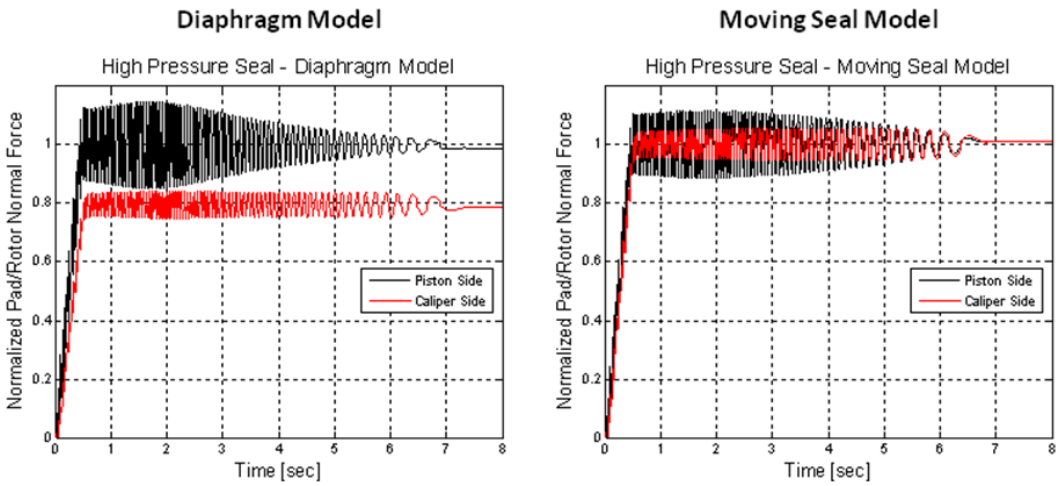

Figure 22: Pad/Rotor Normal Forces vs. Time for Various High Pressure Seal Models

A more realistic output would not have the mean value of the normal forces equal, as the pressure generated in the piston chamber acts through different mechanical components on the caliper side vs. the piston side. The diaphragm model again appears superior in capturing the realistic behavior of the high pressure seal.

5.7. Piston Chambers

The disc-caliper brake system modeled contains two separate pistons, corresponding to two different piston chambers. These chambers share a common hydraulic fluid input and are connected via a thin channel; a schematic of this can be seen back in Figure 14. Both chambers as well as the thin channel are made out of the same material and are cast as one solid piece.

The most realistic model would contain two separate volume elements with a corresponding rigid connection between the two. The initial AMESim model did just this, but computational errors as well as lengthy CPU times resulted. The simulation was thus impractical

for sensitivity analysis. Figure 23 displays the original AMESim model for the piston chambers with labeled components.

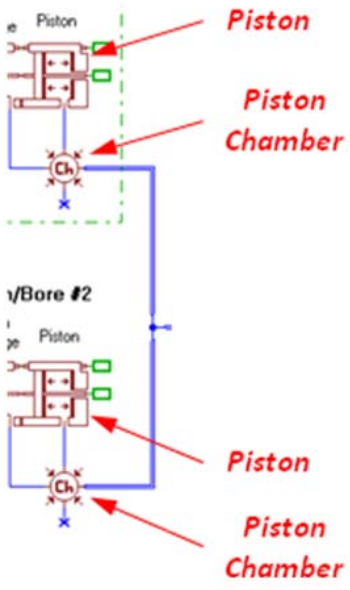

Figure 23: Original AMESim Model for the Piston Chambers

5.8. Piston Chambers – Eigenvalue Analysis

An eigenvalue analysis of the original model revealed a pair of natural frequencies in the kHz range; this is over 10 orders of magnitude greater than the 1st mode of the system. These two modes will be referred to as the 3rd and 4th modes of interest, respectively. Such a large variation is natural frequencies results is a very stiff system, which then leads to long CPU times.

As with all other components, the most pragmatic solution was sought to properly model the piston chambers. Due to the large CPU time, a simplified solution had to be found for the piston chambers that maintained the same representation as the complex model and eliminated the high frequency eigenvalues. Since eigenvalues are a characteristic trait of any

system, all modes in the 0 to 25 Hz range should be retained, as that is the frequency range of interest. There are two modes within this range for the disc-caliper brake model.

The solution sought was to combine the two piston chambers into one single element with a representative volume, including that of the two chambers and connecting channel. Figure 24 displays the improved AMESim model for the piston chambers with labeled components.

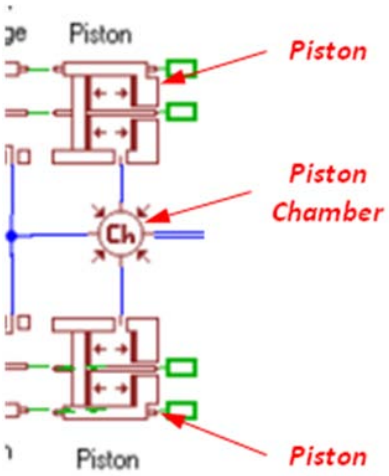

Figure 24: Improved AMESim Model for the Piston Chambers

An eigenvalue analysis of the improved model revealed that the kHz modes had been reduced by over an order of magnitude, though they are still very high frequencies, and the two modes within the 0 to 25 Hz range were not significantly affected. The improved model had successfully reduced the stiffness of the system and produced a reasonable CPU time for sensitivity analysis. A summary of the eigenvalues for both models can be seen in Table 3.

Table 3: Summary of the Eigenvalue Analysis of Both Piston Chamber Models

Model	1st Mode of Interest [Hz]	2nd Mode of Interest [Hz]	3rd Mode of Interest [Hz]	4th Mode of Interest [Hz]
Dual Piston Chamber	4.0	19.2	530600	563700
Single Piston Chamber	4.0	19.9	46490	47020

5.9. Abutment Stiffness Model

In the original formulation of the AMESim model, no abutment stiffness was included as it was an additional complication into an already complex system. However, experimental torque histories of brake systems contained a stick-slip type phenomenon. An accurate model should be able to capture this, and it was hypothesized that the brake pad and knuckle interaction, labeled as the abutment stiffness, is the cause of the stick-slip phenomenon. The brake pad/anchor interaction is that of two dry surfaces rubbing against each other, i.e. Coulomb friction. It should thus be modeled with a representative coefficient of friction as well as a contact stiffness.

5.10. Abutment Stiffness Model – Brake Torque Output

The initial abutment stiffness model included a lumped stiffness model and Coulomb friction element, which multiplied N_{pist} and N_{calp} by a measured coefficient of friction. The normalized brake torque output T(t) for this model can be seen in Figure 25.

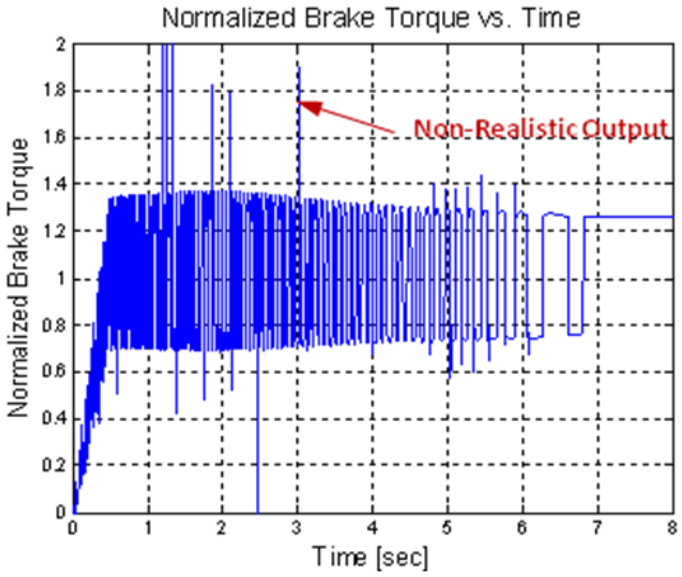

Figure 25: Original Abutment Stiffness AMESim Model T(t) Output

A non-realistic output results from the simulation, as is labeled. Reasons lie in neglecting a maximum attainable Coulomb friction force. In order to correct this error, a saturation level was placed on N_{pist} and N_{ca}; this limit was obtained experimentally. The normalized brake torque output T(t) for the modified AMESim model can be seen in Figure 26.

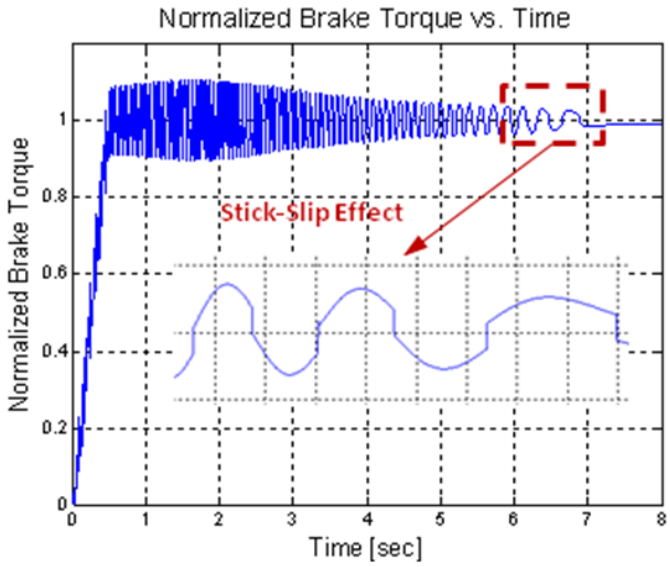

Figure 26: Modified Abutment Stiffness AMESim Model T(t) Output

A realistic output is now obtained, and the stick-slip effect sought is evident. Stick-slip phenomenon occurs at low velocities during Coulomb friction. To better illustrate that the model accurately represents the effect, a plot of normalized brake torque T(t) and disc rotational speed Ω(t) vs. time is shown in Figure 27; the stick-slip is indeed only present at low velocities.

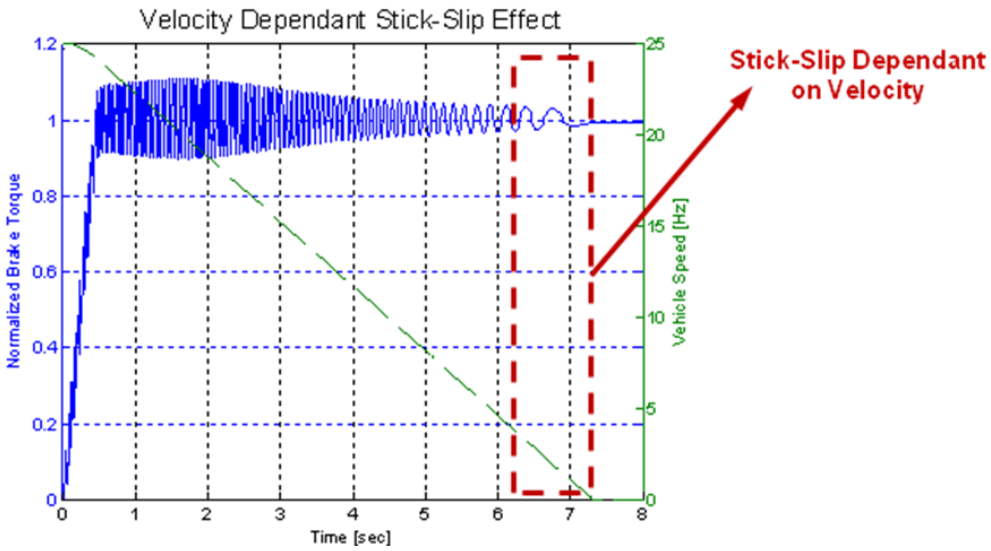

Figure 27: T(t) and Ω(t) Comparison to Illustrate Stick-Slip Phenomenon

6. TYPICAL PARAMETRIC STUDIES

6.1. Method Used

A sensitivity analysis was done for each individual parameter within the AMESim model to determine its effect of the dynamic torque T(t) as well as BTV. A three tier analysis was done with a low, medium, and high level set for each parameter value. The baseline value of the parameter, i.e. the actual value, was then designated as either the low, medium, or high value. The default selection was the medium tier, unless the parameter could not physically be larger or smaller; the remaining two tiers were then assigned a value.

With all three tiers designated, the simulation was then run at each value. The mean BTV as well as the peak-to-peak (PP) BTV was calculated for each tier. This was not done for the entire T(t) time history, but only the portion after the pressure ramp; this is the vibratory portion of interest. A graphical representation of this can be seen in Figure 28. MATLAB script was used to identify the correct portion of T(t) to evaluate, as well as perform the calculations.

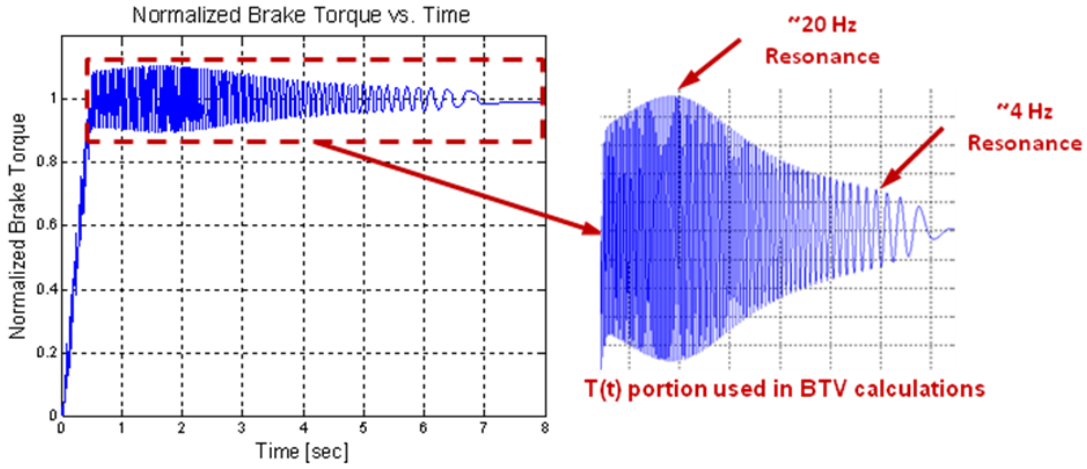

Figure 28: T(t) Portion Used in BTV Calculations for Sensitivity Analysis

Figure 28 displays the answer to the first fundamental question proposed. The simulation does in fact predict a resonance in the 10 to 20 Hz range; it is the 2nd mode of the system and is ~20 Hz. The sensitivity analysis described was used to investigate the remaining fundamental questions.

6.2. Amplitude of DTV

An important question to pose from the standpoint of brake judder analysis is the sensitivity of BTV to DTV, i.e. the amplitude of the sine wave input y(t) at each brake pad. Currently, expensive manufacturing procedures are used to minimize the amplitude as much as possible. It is therefore worthwhile to analyze the improvement of BTV gained from the

expense put into rotor manufacturing. Figure 29 displays the results of the sensitivity analysis for the piston side DTV amplitude; brake torque T(t) is normalized to the baseline value predicted.

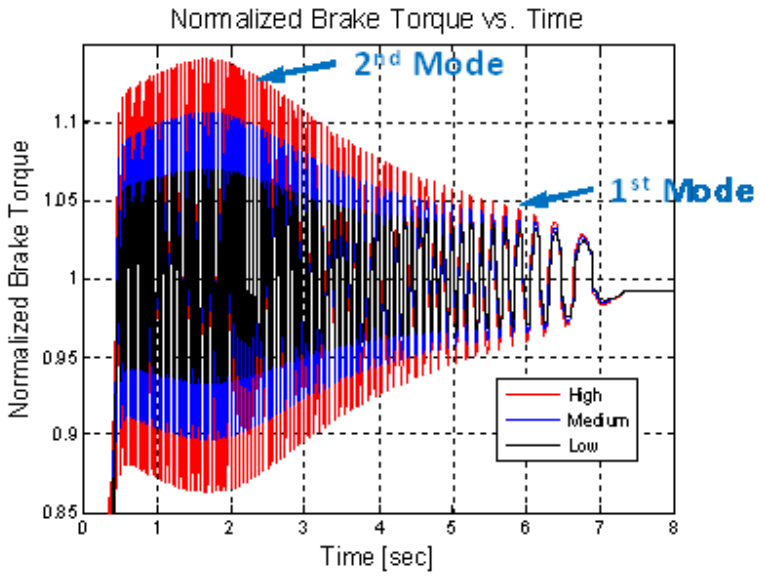

Figure 29: T(t) Output for Piston Side DTV Sensitivity Analysis

It can be seen that an increase in DTV does in fact cause an increase in BTV; normalized mean BTV and peak-to-peak (PP) BTV values can be seen in Table 4. There is over a 30% variation in PP BTV between runs, which is quite significant. The frequency of the first two modes is also tabulated in Table 4; they do not change. As eigenvalues (modes) are an inherent property of the system and thus independent of the input, it logically makes sense that a change in y(t) input would not alter them.

Table 4: Piston Side DTV Sensitivity Analysis Summary

Normalized Piston Side DTV	Normalized Mean BTV	Normalized PP BTV	1st Mode [Hz]	2nd Mode [Hz]
0.5	0.711	0.654	4.00	19.95
1	1.000	1.000	4.00	19.95
1.5	1.317	1.329	4.00	19.95

6.3. Run Out vs. DTV

As seen back in Figure 2, DTV is characterized by the brake pads moving out-of-phase with each other, while run out is when they move in-phase. Of the two, DTV is identified as the main contributor to BTV in all literature reviewed [1-2, 4-5]. Thus, current manufacturing standards for rotor discs emphasize reduction in DTV with little attention paid to run out.

It is thus important to understand and predict what impact run out actually has on BTV in order to better refine manufacturing practices. Rather than perform the three tier sensitivity analysis discussed, a direct comparison was made between DTV and run out; it can be seen in Figure 30. The amplitude of y(t) was identical for both cases, and the direction of the piston brake pad was merely reversed to change the relative phase of the pad movements.

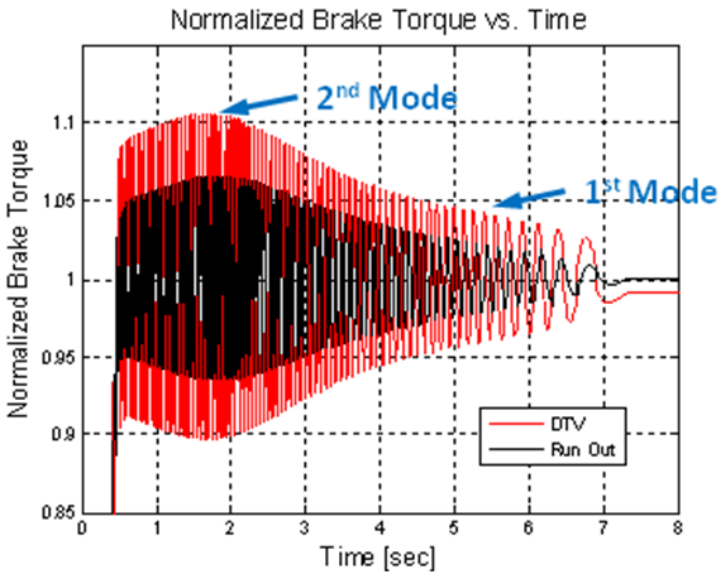

Figure 30: T(t) Output Comparison for DTV vs. Run Out

It can be seen that an increase in run out does cause brake torque variations, but to a lesser extent than DTV. Normalized values of the T(t) output can be seen in Table 5; run out produces roughly 60% of the BTV that is produced by DTV. The decision to focus manufacturing techniques on DTV reduction is thus justified. The first two modes again remain unchanged between the two, as the system itself was not being changed. Only the inputs were altered.

Table 5: Run Out vs. DTV BTV Sensitivity Analysis Summary

	Normalized Mean BTV	Normalized PP BTV	1st Mode [Hz]	2nd Mode [Hz]
DTV	1.000	1.000	4.00	19.95
Run Out	0.625	0.627	4.00	19.95

6.4. Caliper Stiffness

A major goal of this research project was to demonstrate a coupling between the hydraulic and mechanical components of the system. One manner of achieving this is to show

that both mechanical and hydraulic parameters influence the same mode of the coupled system. Thus a sensitivity analysis was done for each parameter in the model, and its effect on the first two modes of the system as well as BTV was observed. One such parameter is the lumped stiffness of the caliper body k_{calp}. The resulting normalized T(t) output for all three tiers can be seen in Figure 31.

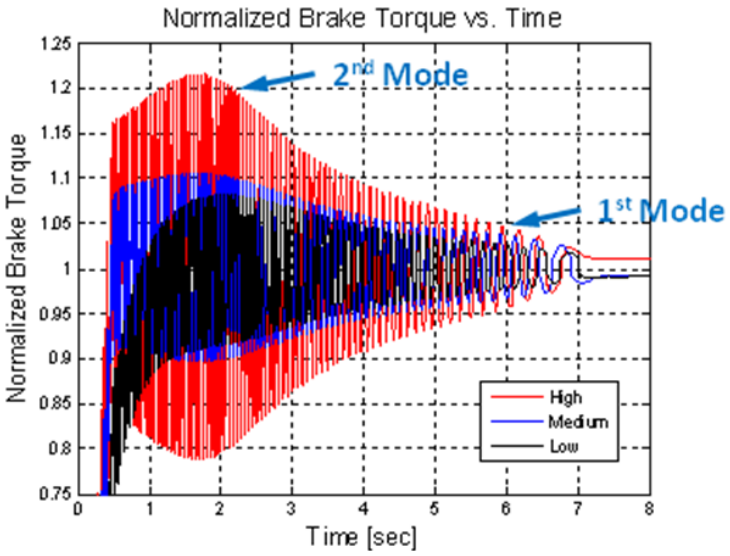

Figure 31: T(t) Output for Caliper Stiffness Sensitivity Analysis

A tabulation of the normalized T(t) results can be seen in Table 6; a higher stiffness generated a higher BTV. The characteristic shape of the T(t) output also changed based on the stiffness value, suggesting a change in the eigenvalues. The frequencies of the first two modes are also tabulated in Table 6 to observe this. The 1st mode varies widely as the caliper stiffness changes, suggesting a strong relationship with k_{calp}, i.e. the 1st mode is dependent on a mechanical parameter.

Table 6: Caliper Stiffness BTV Sensitivity Analysis Summary

Normalized Caliper Stiffness	Normalized Mean BTV	Normalized PP BTV	1st Mode [Hz]	2nd Mode [Hz]
0.1	0.720	0.822	**0.44**	19.81
1	1.000	1.000	**4.00**	19.95
10	1.829	2.039	**18.04**	19.94

6.5. Piston Stiffness

Another mechanical component investigated was the stiffness of the pistons k_{pist}. The resulting normalized T(t) output for all three tiers can be seen in Figure 32.

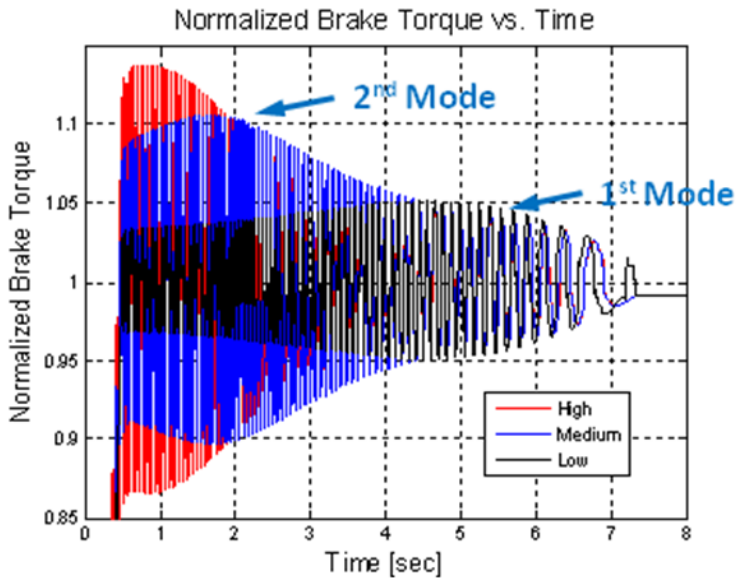

Figure 32: T(t) Output for Piston Stiffness Sensitivity Analysis

A tabulation of the normalized T(t) results can be seen in Table 7. Again, a higher stiffness generated a higher BTV, and the characteristic shape of the T(t) output changed based on the stiffness value. The frequencies of the first two modes are also tabulated in Table 7 to observe this. Unlike with the caliper stiffness, the 1st mode remains unaltered while the 2nd

mode now varies widely as the piston stiffness changes. Therefore, the 2nd mode is also dependant on a mechanical parameter.

Table 7: Piston Stiffness Sensitivity Analysis Summary

Normalized Piston Stiffness	Normalized Mean BTV	Normalized PP BTV	1st Mode [Hz]	2nd Mode [Hz]
0.1	0.553	0.481	3.86	**15.04**
1	1.000	1.000	4.00	**19.95**
10	1.048	1.287	4.02	**22.14**

6.6. Elastic Hose Length

In order to demonstrate a hydraulic and mechanical coupling, hydraulic parameters also needed to be investigated. One such parameter was the length of the elastic hose; the elastic hose is connected directly to the piston chamber. The sensitivity analysis described above was performed, and the resulting normalized T(t) output for all three tiers can be seen in Figure 33.

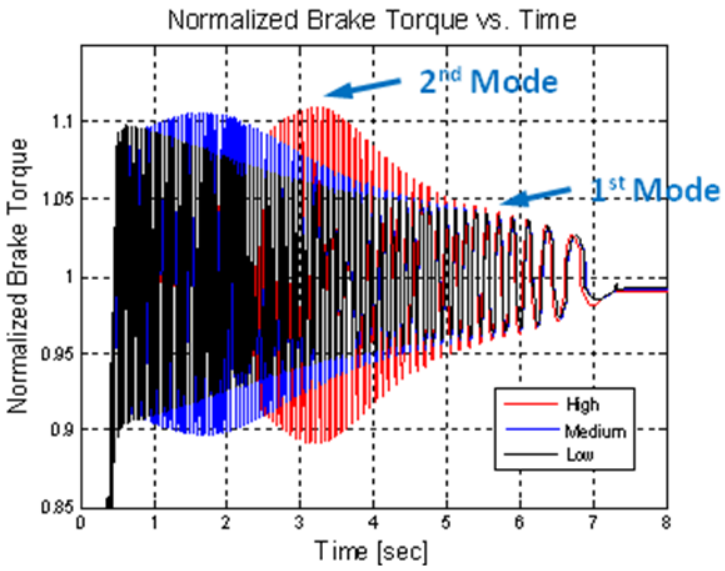

Figure 33: T(t) Output for Elastic Hose Length Sensitivity Analysis

A tabulation of the normalized T(t) results can be seen in Table 8; the values are inconclusive. Overall, the variations in both mean and peak-to-peak BTV are small between the three tiers, and no definitive trend is evident. However, the characteristic shape of the T(t) output varies and can provide insight into the effect of the hose length. The frequencies of the first two modes are also tabulated in Table 8 to observe this. As with the piston stiffness, the 1st mode remains unaltered while the 2nd mode now varies widely as the elastic hose length changes. Therefore, the 2nd mode is dependent on a hydraulic parameter.

Table 8: Elastic Hose Length Sensitivity Analysis Summary

Normalized Elastic Hose Length	Normalized Mean BTV	Normalized PP BTV	1st Mode [Hz]	2nd Mode [Hz]
0.5	0.871	0.934	3.98	**24.67**
1	1.000	1.000	4.00	**19.95**
2	0.941	1.039	4.03	**14.85**

6.7. Summary of Component Parameter Effect on 1st and 2nd Modes

Through the sensitivity analysis, it has been demonstrated that the 2nd mode of the system is dependent on both the mechanical piston stiffness parameter, as well as the hydraulic elastic hose length parameter. The model thus suggests that there is in fact a coupling between the hydraulic and mechanical components in the disc-caliper brake system.

The sensitivity analysis was done for each parameter within the AMESim model, and Figure 34 summarizes the corresponding effect of each parameter on the first two modes of the system. The guide pin viscous damping is represented by g_{cpin}, and a lumped stiffness term k_{hyd} represents the contribution of all hydraulic components. It includes the elastic hose length and

diameter, the diaphragm seal stiffness, the hydraulic chamber, etc. The lumped parameter is merely for visual purposes and not for mathematical calculations.

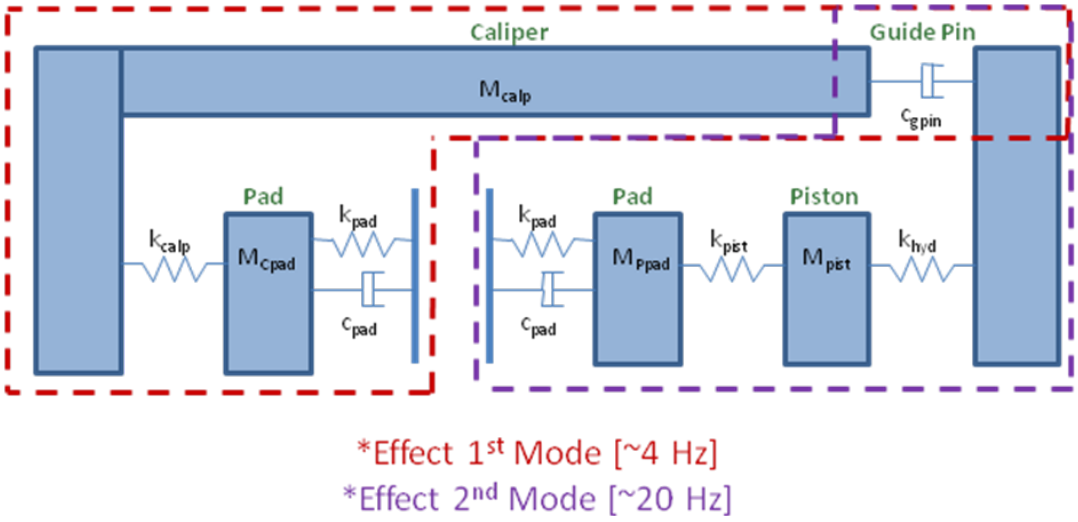

Figure 34: Summary of Component Effect on 1st and 2nd Modes

The caliper side brake pad parameters, caliper stiffness, and guide pin viscous damping all effect the 1st mode of the system. These are all mechanical components, and thus no coupling is present. The piston side brake pad parameters, piston stiffness, lumped hydraulic stiffness, and guide pin viscous damping all effect the 2nd mode of the system. There are mechanical and hydraulic components; therefore coupling is present.

6.8. Addition of an Accumulator

The final fundamental question posed was to investigate the effect of adding an accumulator to the hydraulic system. It is hypothesized that inclusion of a large accumulator will reduce brake pressure variations in the system, thus reducing BTV. A commercially available gas bag accumulator such as the one seen in Figure 35 would be used. The fluid pressure in the accumulator is defined as P_{app}, while the pre-charge pressure of the gas bag is defined as P_{gas}.

The fluid flow rate is defined by Q. Figure 35 also shows the location of the accumulator in the hydraulic system; it is proposed to place it directly before the piston chamber.

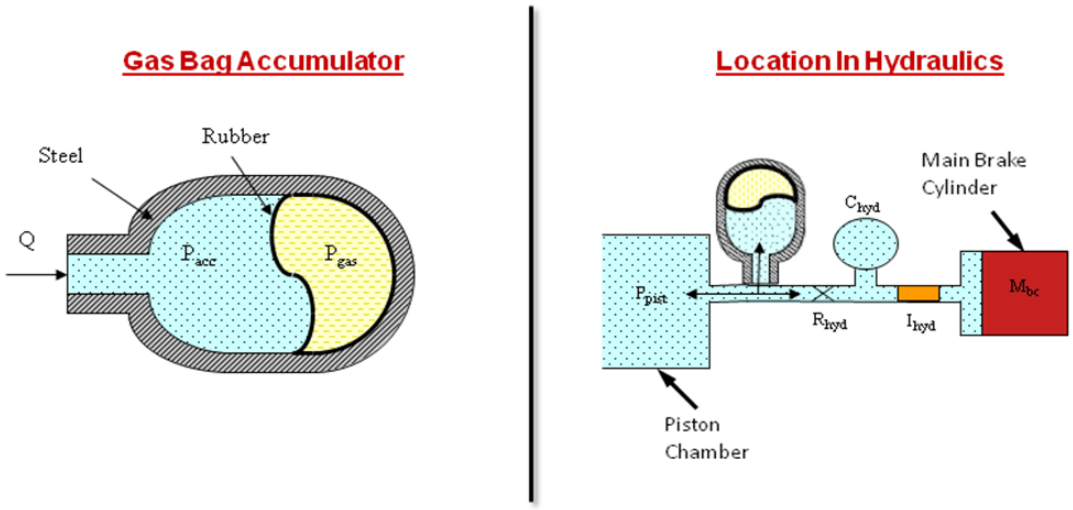

Figure 35: Gas Bag Accumulator Schematic and Location in Hydraulic System

AMESim has a gas bag super-component available within its library. The user can specify its volume, inlet orifice size, and pre-charge pressure. The AMESim model with the gas bag super-component incorporated can be seen in Figure 36. A direct connection hydraulic line model was used to place the accumulator directly at the piston chamber, as seen in Figure 35.

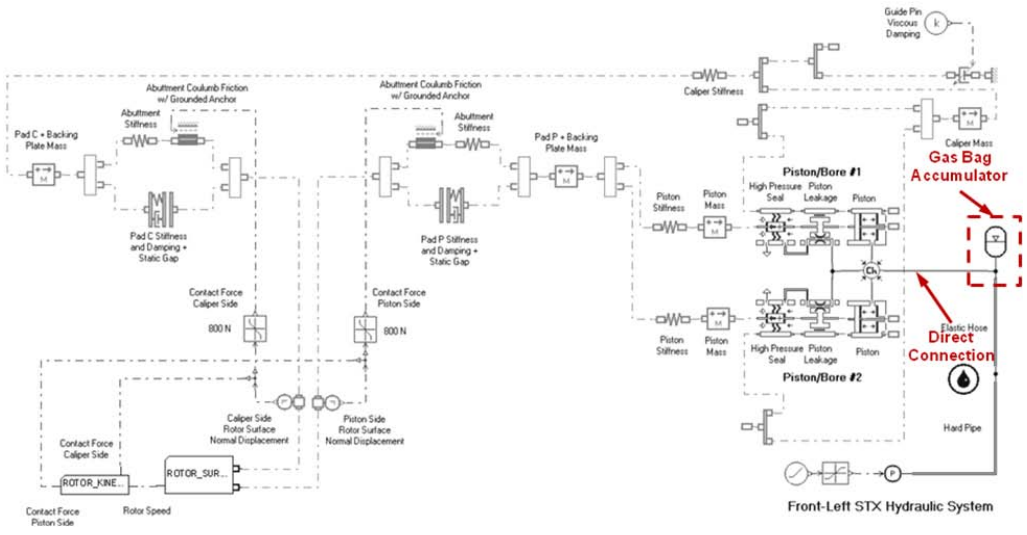

Figure 36: AMESim Model with Added Gas Bas Accumulator

A variety of different accumulator configurations were experimented with in an effort to examine the effect on BTV. Two specific examples were a 0.25 L accumulator and a 0.50 L accumulator with a 15 bar pre-charge for each. Figure 37 shows the normalized T(t) output with a 0.25 L accumulator; Figure 38 shows the normalized T(t) output with a 0.50 L accumulator. Both are compared to the normalized T(t) output with no accumulator.

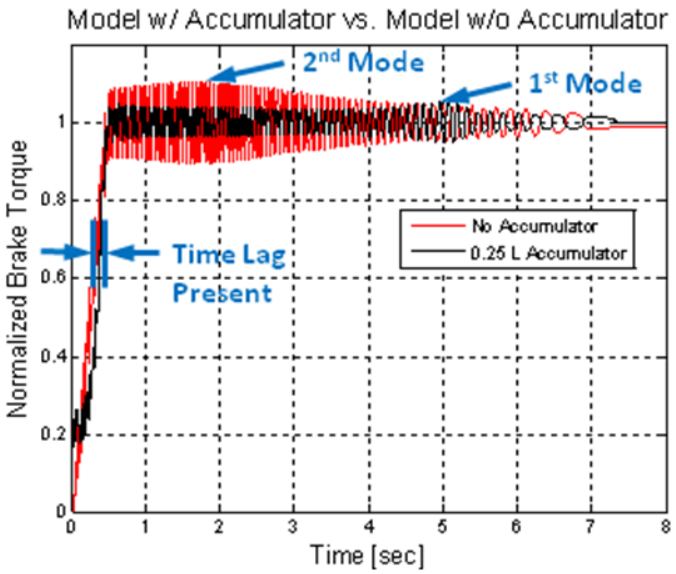

Figure 37: Comparison of T(t) Output for No Accumulator vs. 0.25 L Accumulator

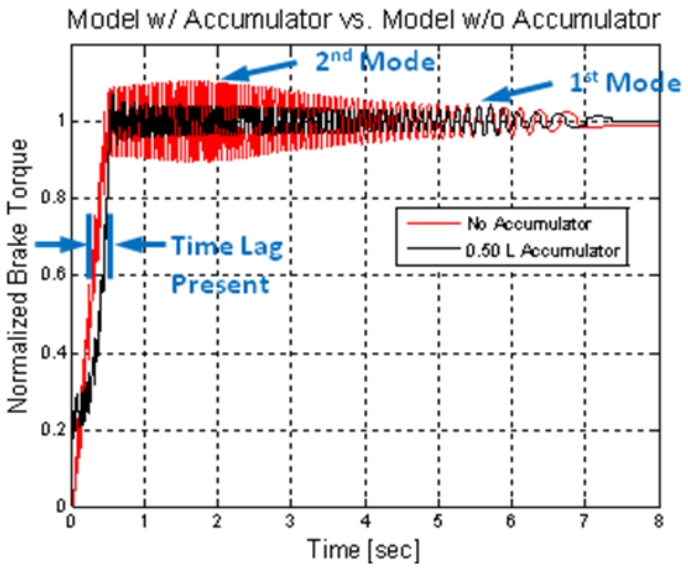

Figure 38: Comparison of T(t) Output for No Accumulator vs. 0.50 L Accumulator

A large reduction in BTV is evident for both accumulators. Normalized values can be seen in Table 9, as well as the frequencies of the first two modes. The 2nd mode is drastically reduced as the size of the accumulator is increased. The BTV decreases as a result of this, since there is no resonance in the higher frequency ranger were larger excitations occur. A detrimental effect with a larger accumulator is an increased time lag in the transient response of the system. Essentially, the brakes will take longer to reach full effect after initial suppression of the brake pedal. This is detrimental to pedal feel and thus customer satisfaction.

Table 9: Accumulator Effect Summary

	Normalized Mean BTV	Normalized PP BTV	1st Mode [Hz]	2nd Mode [Hz]
No Accumulator	1.000	1.000	4.00	19.95
0.25 L Accumulator	0.511	0.555	3.99	8.89
0.50 L Accumulator	0.491	0.505	3.98	6.62

7. CONCLUSION

7.1. Summary

A new multi-physics software AMESim Image.Lab was used to formulate a coupled mechanical and hydraulic model of an automotive brake system [7]. Specifically, a floating disc-caliper type brake system was analyzed. Using the model and a three tier sensitivity analysis of the system parameters, several fundamental questions were posed, investigated, and answered.

First, it was demonstrated that the model does in fact predict a resonance (mode) in the 10-20 Hz range associated with judder in the literature reviewed [2]. The mode is at roughly 20 Hz and is the 2^{nd} mode of the system. The value of this mode varies widely depending on parameter selection.

The correlation between the amplitude of DTV and the amount of BTV generated was also investigated. It was found that larger amplitudes led to larger brake torque variations. DTV is defined when the brake pads move out-of-phase with each other; run out is when they move in-phase. The comparison of DTV input vs. run out input was conducted to determine which causes greater BTV. It was found that run out causes only 60% the BTV that DTV does for a given y(t) amplitude and pressure applied $P_A(t)$.

A major goal of the model was to demonstrate a coupling between the mechanical and hydraulic components in the system. The three tier sensitivity analysis conducted was used to explore how each parameter influenced the first two modes of the system. It was found that only mechanical components effected the 1^{st} mode (~4 Hz), but both mechanical and hydraulic

components effected the 2nd mode (~20 Hz). The model thus suggests a mechanical and hydraulic coupling.

The final fundamental question investigated was how the addition of an accumulator into the hydraulic system would affect T(t). It was proposed to place a commercially available gas bag accumulator directly at the piston chamber in hopes of reducing BPV, thus mitigating BTV. It was found that the brake torque variations in fact were decreased by roughly 50%, but a loss in pedal feel also resulted.

7.2. Recommendations for Future Work

It should be noted that no experimental validation has been conducted on the AMESim model. This will be the top priority for future work. The current model results have provided some insight into each parameters influence on T(t) and given direction for experimental tests. All fundamental questions must be experimentally investigated, particularly the mechanical and hydraulic coupling; the elastic hose length and piston side brake pad stiffness will be the basis for tests.

Non-linearities should be added to the model as is necessary. The pad stiffness k_{pad} and damping coefficient c_{pad} are known to be nonlinear and must be determined experimentally [4]. The pad coefficient of friction μ_{pad} is also known to be nonlinear. Accurate formulation of non-linear models can be difficult, thus only those deemed essentially to model behavior will be included. The experimental validation tests will be the basis for evaluating key non-linearities.

The abutment stiffness model will also be refined as the research progresses. Rough experimental methods with low accuracy were used to initially identify the Coulomb coefficient of friction as well as the max frictional force. These values are likely non-linear, and should properly be characterized for an accurate representation of the stick-slip phenomenon observed in experimental results.

Finally, an alternative disc-brake caliper design should be investigated. It is a fixed caliper design, as opposed to the floating caliper design. A picture will key components labeled can be seen in Figure 39. This design contains pistons on both sides of the rotor surface as opposed to one side with the floating caliper design. The caliper now remains fixed, and only the hydraulic system reacts to the y(t) input at each pad.

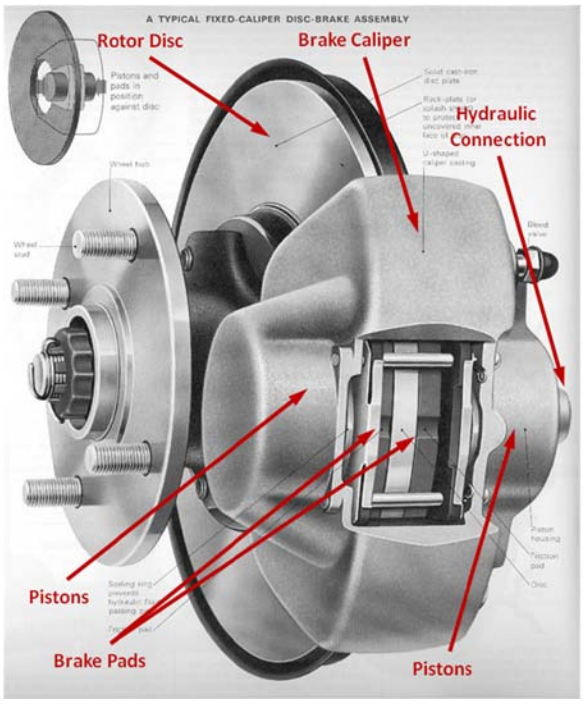

Figure 39: Typical Fixed Disc-Caliper Brake Assembly [8]

ACKNOWLEDGEMENTS

1) My advisor, Dr. Rajendra Singh, for his knowledge and guidance throughout the project.

2) Dr. Bill Post and Honda R&D for funding the project and inputting their knowledge and experience into the direction of the project.

3) LMS© for providing the AMESim software used.

4) The Ohio State College of Engineering for providing a scholarship for my research

5) The Institute of Noise Control Engineering for providing a scholarship for my research

6) Dr. Jason Dreyer and the rest of the Brake Judder Improvement Team for working hand in hand with my research project through their own research focuses.

REFERENCES

[1] A. Leslie, “Mathematical Model of Brake Caliper to Determine Brake Torque Variation Associated with Disc Thickness Variation (DTV) Input”, SAE Paper No. 2004-01-2777, 2004.

[2] H. Jacobsson, “Disc Brake Judder Considering Instantaneous Disc Thickness or Spatial Friction Variation”, IMechE Journal of Automobile Engineering, 217, 325-342, 2003.

[3] Doebelin, O., “System Dynamics Modeling and Response,” Friedr. Vieweg & Sohn Verlag, Wiesbaden, 2006, pg 96.

[4] J Kang and S Choi, “Brake Dynamometer Model Predicting Brake Torque Variation to Disc Thickness Variation”, IMechE Journal of Automobile Engineering, 221, 49-55, 2007.

[5] H. Jacobsson, “Aspects of Disc Brake Judder”, IMechE Journal of Automobile Engineering, 217, 419-430, 2003.

[6] R. Singh, Personal Conversations on Brake Judder, August 2009.

[7] LMS International. “1D Multi-Domain System Simulation.” 2009. 1 April 2009. http://www.lmsintl.com/imagine-amesim-1-d-multi-domain-system-simulation

[8] B. Breuer and K. H. Bill, “Brake Technology Handbook,” W. W. Norton & Company, New York, 1977, pg 110.